Atomistic Modeling of Native Point Defects in Yttrium Aluminum Garnet Crystals

Maija M. Kuklja[†] and Ravindra Pandey

Department of Physics, Michigan Technological University, Houghton, Michigan   49931

Native point defects in yttrium aluminum garnet (YAG) are studied in the framework of the pair-potential approximation, coupled with the shell-model description of the lattice ions. For the perfect lattice, a new set of potential parameters is obtained; these parameters reproduce the structure, elastic, and dielectric constants of YAG very well. The calculated formulation energies for native defects suggest that antisite disorder is preferred over Frenkel and Schottky-like disorder in YAG. The calculated values of the distortion that is caused by the antisite Y atom that substitutes in the Al site in the lattice are in excellent agreement with the extended X-ray absorption fine-structure (EXAFS) measurements. In nonstoichiometric YAG, the calculated reaction energies indicate that excess Y_2O_3 or Al_2O_3 most likely is accommodated by the formation of antisites, rather than vacancies, in the lattice.

I. Introduction

YTTRIUM ALUMINUM GARNET (YAG) is an important material whose technological applications range from lasers to propulsion systems. For example, Nd^{3+}-doped YAG is a well-known laser material, whereas the YAG:Al_2O_3 composite is an ideal material for high-temperature structural-ceramic applications.[1] Over the years, most experimental efforts have been focused on understanding the optical[2–6] and magnetic[7–10] properties of dopant ions in the YAG lattice. Relatively less attention has been given to investigate its properties for the purpose of exploiting its potential in high-temperature applications.[11–13]

The diffusion and defect chemistry of pure and doped YAG have been the subject of a few experimental and theoretical studies.[3,14–18] An analysis of electroconductivity measurements and diffusion coefficients on a series of the crystals with the garnet structure has established that YAG is an ionic conductor.[14] However, for high temperatures, the situation changes and, as it has been suggested, the conductivity of YAG exhibits mixed ionic–electronic character[14] for temperatures >800°C. A similar conclusion also was achieved from the study of transport properties and defect formation of calcium- and magnesium-doped YAG.[16]

A theoretical study based on the shell model has considered only the presence of vacancies and interstitials in the lattice, predicting the dominance of vacancies over interstitials.[17] However, spectroscopic study of stoichiometry deviation in YAG has shown a possibility of cation antisite substitution in the garnet crystal lattice.[19] This observation has been confirmed very recently via extended X-ray analysis fine-structure (EXAFS) measurements[20] in Y_2O_3-rich YAG, which identifies the local order around the Y antisite atoms. Furthermore, the atomistic study of defects in yttrium iron garnet (YIG) that was performed by Donnerberg and Catlow[21] also concluded that antisites, rather than vacancies, would dominate the intrinsic disorder in this material.

YAG and YIG materials are very similar; therefore, it is expected that antisites are likely to have an important role in YAG and should be considered in any experimental or theoretical study of its defect chemistry. In this paper, we attempt to perform such a task by reporting the results of a theoretical study of native defects in YAG. Our approach is based on the pair-potential and shell-model description of the ionic interactions in the crystalline lattice, for which we will determine a new set of potential parameters. Then, this set will be used to study the intrinsic disorder and reactions that describe the deviations from stoichiometry in YAG.

II. Method

Partitioning of a crystalline lattice into two regions is the basis of the cluster model, which is applied very often in calculations of defect properties in ionic materials. The main idea is to separate a cluster (referenced as region 1) from the rest of the lattice (referenced as region 2). Also, the perturbation that is caused by the defect in the crystal is assumed to be negligibly weak beyond the cluster. The cluster generally consists of a limited region that contains defects and several spheres of its nearest surroundings. The number of ions in the cluster varies from situation to situation and is dependent on the type of defects in the system. In calculations, the cluster is treated explicitly within a selected method, whereas the remainder of the lattice (represented by region 2) is treated appropriately. Thus, the crystal lattice energy can be written in the form[22]

$$E = E_1(\vec{x}) + E_2(\vec{x}, \vec{\xi}) + E_3(\vec{\xi}) \tag{1}$$

where E is the total energy of the crystal, $E_1(\vec{x})$ the cluster energy, and $E_3(\vec{\xi})$ the energy of the outer region. $E_2(\vec{x}, \vec{\xi})$ is the energy of the interaction between regions 1 and 2, depending on both ion coordinates of the cluster $\vec{x}$ and the rest of the crystal $\vec{\xi}$. The exact expression for the crystal energy can be written as a series of interaction terms that contain n body components. The interionic potential model that has been used in the present work is well described elsewhere (see, for example, Catlow and co-workers[22,23] and Norgett and co-workers[24,25]). Therefore, here, we discuss only the primary ideas, rather than give a detailed description. The method assumes that the total crystal energy can be given as a sum of all pairwise interactions in the lattice. In other words, all terms but

the two-body contribution are neglected in the series. Then, one can write

$$E = \sum_{i>j} E(i,j) \tag{2}$$

where

$$E(i,j) = \phi_{ij}(r_{ij}) + \frac{q_i q_j}{r_{ij}} \tag{3}$$

$E(i,j)$ is the energy of the interaction between ions i and j, with charges q_i and q_j located at a distance r_{ij}. The term $\phi_{ij}(r_{ij})$ is a suitable pair potential that describes the short-range interaction between ions. The latter is a result of atom repulsion that is due to their electron-shell overlapping and dispersion attraction. For ionic materials, this term generally has the form of a Buckingham potential:[26]

$$\phi_{ij}(r_{ij}) = A_{ij} \exp\left(-\frac{r_{ij}}{\rho_{ij}}\right) - \frac{C_{ij}}{r_{ij}^6} \tag{4}$$

A_{ij}, ρ_{ij}, and C_{ij} are empirical parameters that usually are fitted to crystalline properties.

The ionic displacements in inner region 1 are obtained explicitly via a minimization of the total energy. For outer region 2, the ionic displacements are determined by the electric field that is due to the effective charge of the defect in the framework of the Mott–Littleton approximation.[27] For cubic materials such as YAG, the ionic displacements are isotropic and are given by[24,25]

$$\delta \vec{x} = \frac{v_c}{4\pi} \left\{ \frac{[(\vec{G}^{-1})\vec{q}](1 - \varepsilon^{-1})}{(\vec{q}^T \vec{G}^{-1} \vec{q})} D^x \right\} \tag{5}$$

in which $\delta \vec{x}$ is a vector of displacements in the x-, y-, or z-directions, v_c the unit-cell volume, D^x the corresponding electric displacement, $\hat{G}$ the second derivative of the non-Coulombic interaction matrix, and ε the trace of the dielectric constant tensor.

The interionic potential model is improved significantly if one considers the electronic polarization that is introduced by the charged defects in the lattice. This consideration can be made using the shell model of Dick and Overhauser,[28] which describes the valence electrons as a massless charged *shell*, that is coupled with the *core* of the ion by isotropic elastic forces. All formulae are still valid if one rewrites them by substituting shell and core charges and coordinates instead of using rigid-ion charges. Both shell and core charges and the coupling constants of a shell and core of the given ion are the parameters of the theory; these parameters generally are derived empirically.

III. Results and Discussion

Experimental studies of garnets started long ago, because the garnet structure originally was solved by Menzer.[29,30] However, there are only a few theoretical investigations that have focused on the defect chemistry in garnets.[17,21,31,32] The garnet structure belongs to the space group $Ia3d$ (O_h^{10}). The cations are all in special positions—labeled as a, c, and d with no positional degrees of freedom—whereas the O atoms are placed in the general positions 96(h). Figure 1 shows the arrangement of cation sites of YAG, in terms of the garnet structure. Y occupies dodecahedral 24(c) positions, whereas there are two different sites for Al ions—namely, octahedral 16(a) and tetrahedral 24(d) in the lattice (see, for example, Wyckoff[33]). This observation leads to the formula $Y_3Al_2Al_3O_{12}$, which is commonly written as $Y_3Al_5O_{12}$. The unit cell is large and consists of eight formula units (160 atoms). For calculations, the O positional parameters in the lattice were taken from neutron-diffraction measurements by Prince[34] and are given by $x = -0.029$, $y = 0.053$, and $z = 0.151$. The X-ray diffraction (XRD) study by Euler and Bruce[35] reported the cation–oxygen distances in YAG to be 1.94 and 1.76 Å for Al^{3+}(a)–O^{2-} and Al^{3+}(d)–O^{2-}, respectively. Following Geller,[36] the most accurate value of the lattice constant for the stoichiometric $Y_3Al_5O_{12}$ is 12.000 ± 0.002 Å. Several other experimental studies have determined the lattice constant to be slightly higher, which may be due to the presence of excess yttrium in the lattice.[36,37]

(1) Interatomic Potentials

For the interatomic potential model, formal ionic charges are assigned to the host-lattice ions—thereby, Y^{3+}, Al^{3+}, and O^{2-}
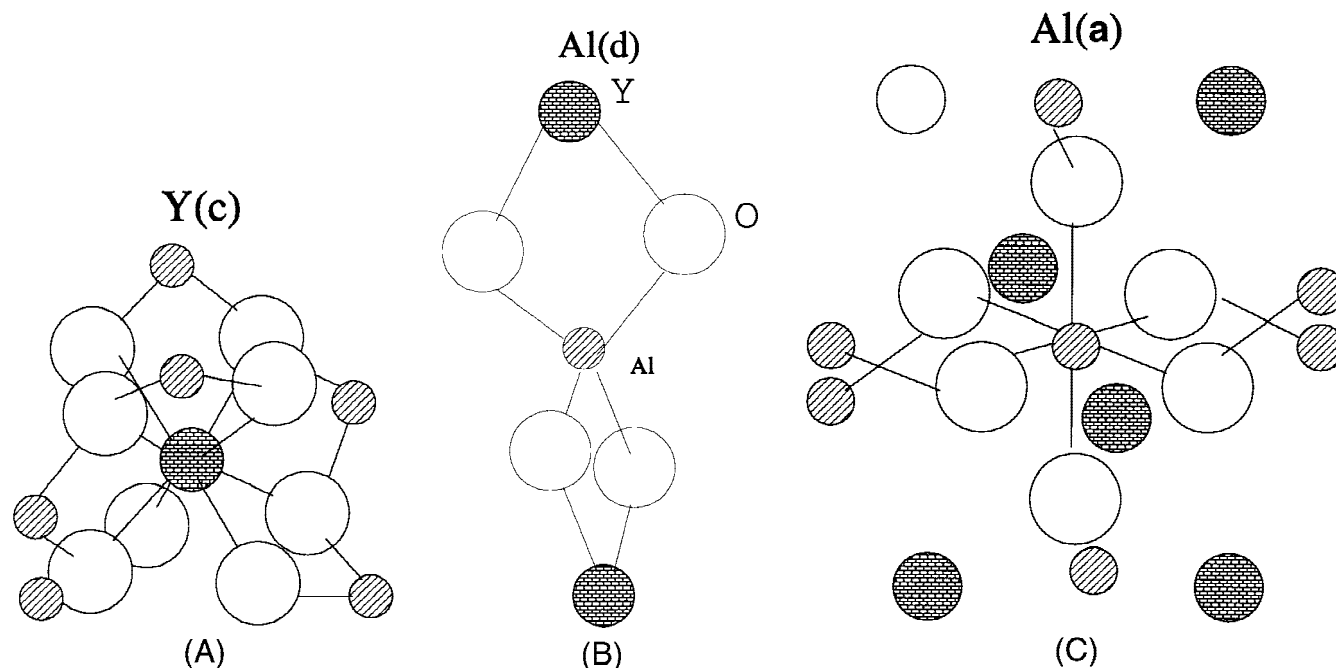
Fig. 1. Schematic representations of the arrangement of YAG, in terms of the garnet structure. The figures depict a fragment of a cluster centered at (A) the Y atom, which is dodecahedrally coordinated (Y(c)), (B) the Al atom that is tetrahedrally coordinated (Al(d)), and (C) the Al atom that is octahedrally coordinated (Al(a)) in the crystal.

in YAG. The short-range interaction terms that are considered in the model describe cation–oxygen and oxygen–oxygen interactions. The short-range interactions between cations are ignored, because they generally become very small for large separations (2.99 Å for d(Y–Al(d)), 3.67 Å for d(Y–Y) and d(Al(d)–Al(d)), and 5.19 Å for d(Al(a)–Al(a)) in YAG).

Note that the parameters for the $O^{2-}-O^{2-}$ interaction are assumed to be transferrable among a series of oxides and are taken from the work of Catlow and co-workers.[22,23,38] These parameters were obtained from Hartree–Fock calculations of the interaction of two negative O anions. Accurate representation of the ionic polarization of a crystalline lattice is known to be very important for defect modeling; therefore, we have considered all the constituent ions of YAG (i.e., Y^{3+}, Al^{3+}, and O^{2-}) as being polarizable ions in the lattice. Then, the model parameters are fitted to experimentally known YAG crystal properties, such as the structure, elastic, and dielectric constants; these parameters are given in Table I. (For details of the fitting procedure, refer to the General Utility Lattice Program (GULP) described by Gale.[39]) Table II shows that the model parameters reproduce the crystalline properties of YAG very well, thus providing a sound basis for extending the model to defect calculations.

Recently, Bush *et al.*[40] obtained a consistent set of pair potentials that were empirically fitted specifically to experimentally measured lattice properties of crystal oxides, including YAG. This set of parameters was in addition to the potential-parameter set that was used earlier by Schuh *et al.*,[17] which was fitted to Al_2O_3 and Y_2O_3 structure properties.[22,41] Although these two sets of interatomic potentials agree well with the experimental values of the lattice structure and elastic constants of YAG, they do not yield the correct low- and high-frequency dielectric constants.

In fact, the respective dielectric constants are overestimated by the first parameter set (16.2 and 4.0) and are underestimated by the second set (8.1 and 2.9), in comparison to the experimental values of 11.0 and 3.5. This discrepancy may be due to different descriptions of cationic polarizability. The Bush set contains rigid Y and polarizable Al cations, and, in contrast, the Schuh set contains rigid Al and polarizable Y cations. On the basis of ionic radii, the Y cation is expected to be more polarizable than the Al cation. Our calculations indicate that an inclusion of both Y and Al polarizabilities into the model allows us to describe the dielectric properties of YAG very well. We note here that an accurate representation of the dielectric constants using the shell model is essential in obtaining reliable defect energies in ionic materials such as oxides.

To further check the adequacy of the derived potential parameters, we examine the stability of the YAG lattice, with respect to its component oxides:

$$3Y_2O_3 + 5Al_2O_3 \rightarrow 2Y_3Al_5O_{12} \qquad (6)$$

$$Al_2O_3 + 3YAlO_3 \rightarrow Y_3Al_5O_{12} \qquad (7)$$
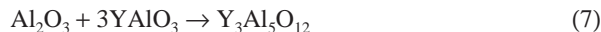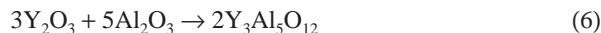
The reaction enthalpies are –2.4 and –1.6 eV, respectively, per YAG formula unit, which indicates that YAG is, indeed, a stable compound. These values are comparable to the corresponding reaction enthalpies for YIG, which are –1.6 and –2.9 eV, respectively.[21]

The structure properties of orthorhombic perovskite-like $YAlO_3$ and the garnet $Y_4Al_4O_{12}$ compound are well reproduced by our potential model. For example, the calculated lattice constants of $YAlO_3$ (a = 5.104 Å, b = 5.260 Å, c = 7.648 Å) agree well with the experimental data (5.179, 5.329, and 7.370 Å, respectively[42,43]). For the cubic $Y_4Al_4O_{12}$, the calculated lattice constant of 12.106 Å is only 0.9% larger than the experimental value of 11.989 Å.[44]

(2) Intrinsic-Defect Structure

For calculations of native point defects in YAG, the lattice was simulated by a large cluster that contained more than 250 ions. The ions that surrounded the defect in the cluster were allowed to relax until a minimum total energy was achieved. The rest of the lattice was considered in terms of a Mott–Littleton approximation.[27] The calculations were performed using the GULP program code.[39]

A vacancy formation was simulated as a removal of a regular lattice-site ion to infinity. To model interstitials, one ion was added to the crystal from infinity and was located in the empty interstitial position in the lattice. In the case of O interstitials, we probed all the possible positions in YAG, which are referred to as f and g.[30] For cations, the b positions were examined. The calculated formation energies for the isolated basic defects (which are collected in Table A-II in the Appendix)

Table I.   Interatomic Potential Parameters and Shell Constants[†]

Ion interaction	A (eV)	ρ (Å)	C (eV/Å^6)	Y^+ (|e|)	K^+ (eV/Å^2)
$O^{2-}-O^{2-}$[‡]	22764.000	0.149	27.88	0.8481	74.92
$Y^{3+}-O^{2-}$	2036.8379	0.3103	0.0	–0.251	46.7288
$Al^{3+}-O^{2-}$	741.9007	0.3566	0.0	0.043	40.8618

[†]Parameters A, ρ, and C are from the Buckingham potential equation (see text, Eq. (4)); Y^+ is the charge of the core, and K^+ is the core–shell spring constant. [‡]Potentials for the $O^{2-}-O^{2-}$ interaction are taken from Lewis and Catlow.[41]
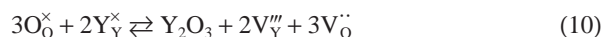
Table II.   Structural Data for Yttrium Aluminum Garnet, Calculated Using Different Interatomic Potential Parameter Sets

Parameter	Value			
	Experiment	Present study	Schuh	Bush
Cohesive energy per formula unit (eV)		–589.28	–602.50	–601.17
Unit-cell/lattice parameters				
a (Å)	12.000[†]	11.988	12.002	12.143
Angle, α (degrees)	90	90	90	90
Unit-cell volume, V (Å^3)	867.45	861.36	869.69	895.15
Density, ρ (g/cm^3)	4.53[‡]	4.58	4.53	4.40
Elastic constants ($\times 10^{11}$ dyne/cm^2)				
C_{11}	33.3[§]	34.0	39.5	33.0
C_{12}	11.3[§]	12.7	13.5	16.5
C_{44}	11.5[§]	11.2	11.7	13.1
Relative permittivities				
ε_0	11.0[¶]	11.4	8.1	16.2
ε_∞	3.5[¶]	3.5	2.9	4.0

[†]From Geller.[36] [‡]From Kitaeva *et al.*[2] [§]From Kitaeva *et al.*[49] [¶]From Hellwege.[50]

now can be used to analyze the energetics of Schottky and Frenkel disorder in the lattice. For the reader's convenience, earlier potential sets[17,40] and defect energies borrowed from Schuh *et al.*,[17] as well as those obtained here using the corresponding set of pair potentials, are given in the Appendix for comparison.

YAG is a complex oxide, and its lattice consists of three sublattices; therefore, the possible Schottky-like structure disorder can be written in the form

$$0 \rightleftarrows 3V_Y''' + 5V_{Al}''' + 12V_O^{\cdot\cdot} \qquad (8)$$

$$3O_O^\times + 2Al_{Al}^\times \rightleftarrows Al_2O_3 + 2V_{Al}''' + 3V_O^{\cdot\cdot} \qquad (9)$$

$$3O_O^\times + 2Y_Y^\times \rightleftarrows Y_2O_3 + 2V_Y''' + 3V_O^{\cdot\cdot} \qquad (10)$$

$$3O_O^\times + Y_Y^\times + Al_{Al}^\times \rightleftarrows YAlO_3 + V_Y''' + V_{Al}''' + 3V_O^{\cdot\cdot} \qquad (11)$$
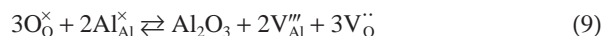
where Kröger–Vink[45] notation has been used to denote defects.

Here, reaction (8) corresponds to the true Schottky disorder and the remaining reactions (reactions (9)–(11)) are given as examples of a change in the chemical composition of the material. They each can be interpreted as a possibility of self-segregation in stoichiometric YAG crystal by the Schottky-like disorder in either of the cation sublattices.

The Frenkel disorder can be written as follows:

$$Al_{Al}^\times \rightleftarrows V_{Al}''' + Al_i^{\cdot\cdot\cdot} \qquad (12)$$

$$Y_Y^\times \rightleftarrows V_Y''' + Y_i^{\cdot\cdot\cdot} \qquad (13)$$

$$O_O^\times \rightleftarrows V_O^{\cdot\cdot} + O_i'' \qquad (14)$$

The computed formation energies (which are collected in Table A-III in the Appendix) suggest that the Schottky-like disorder seems to be more favorable than the Frenkel disorder. Nevertheless, even Schottky defect formation demands a rather-high energy (~3.9–4.7 eV per defect). Therefore, we can suppose that neither Frenkel and Schottky defects are likely to occur in YAG. This conclusion is consistent with the results that have been reported by Donnerberg and Catlow[21] for YIG crystals. Furthermore, the large enthalpies of reactions (9)–(11) preclude the occurrence of self-segregation in stoichiometric YAG crystal, as also observed experimentally.[46]

Next, we consider antisite disorder in the cation sublattice of YAG, which can be described as follows:

$$Y_Y^\times + Al_{Al(a)}^\times \rightleftarrows Y_{Al(a)}^\times + Al_Y^\times \qquad (15)$$

$$Y_Y^\times + Al_{Al(d)}^\times \rightleftarrows Y_{Al(d)}^\times + Al_Y^\times \qquad (16)$$

The corresponding antisite-pair formation energy is estimated to be ~0.9 and ~1.8 eV per defect for reactions (15) and (16), respectively, which suggests that the antisite disorder is preferred over Schottky and Frenkel disorder in YAG. We note here that the Y cation prefers to be located at the Al(a) site rather than the Al(d) site. This observation is expected, based on the coordination numbers of these ions in the lattice: the Y cation has coordination number of eight, whereas Al(a) and Al(d) cations have six and four nearest-neighbor O ions, respectively (see Fig. 1). Antisite-pair formation in the perovskite-like YAlO₃ compound also requires a very low energy (0.62 eV per defect), which indicates that these defects should have an important role in the material.

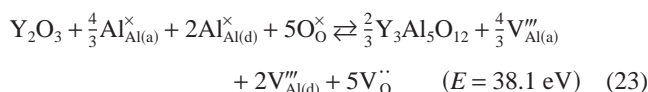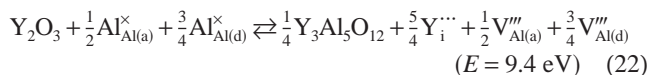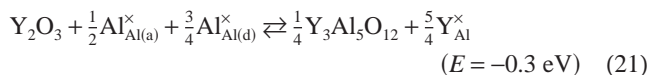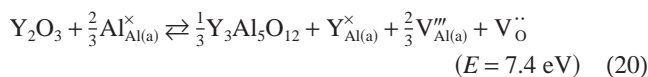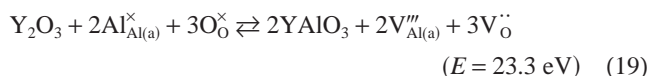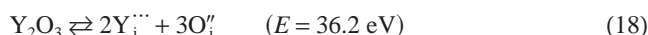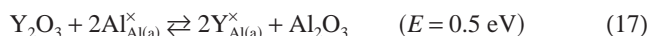Experimental studies performed by Ashurov *et al.*,[19] in fact, suggested that the Y cation can occupy its regular dodecahedral site as well as the Al(a) site in YAG. Those authors investigated nonstoichiometric $Y_3(Y_xAl_{2-x})Al_3O_{12}$ crystals by measuring the spectra of rare-earth impurity ions in the lattice and concluded that the substitution of the Y cation at the Al(a) site introduces the lattice distortion. Recent X-ray absorption near-edge structure (XANES) and EXAFS measurements by Lan-

dron *et al.*[20] investigated the local order around Y regular and antisite locations in Y_2O_3-rich YAG. As it was shown, an increase of the electronegativity of the site ions after the substitution of Al cations by Y cations implies that the oxygen bond in the lattice becomes less ionic. This results in the shortening of the distance between Y and O (d(Y–O)), from 2.43 Å to 2.10 Å, and this new shortened distance is now similar to the mean d(Y–O) distance of the Y cation in the octahedral position in Y_2O_3. From our calculation, the substitution of the Y cation at the Al(a) site in the YAG lattice is accompanied by a decrease in d(Y–O) to 2.08 Å, which is in excellent agreement with the experimental value of 2.10 Å.[20]
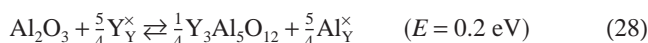
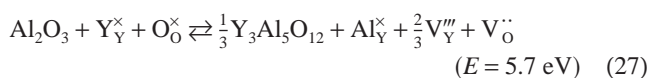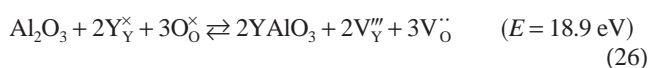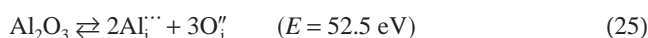### (3) Deviations from Stoichiometry

Although experimental studies long ago identified the presence of nonstoichiometric phases in YAG, the mechanism by which an excess of Y_2O_3 or Al_2O_3 can be accommodated in the lattice is not completely understood. In early work on gallium and aluminum garnets,[37] excess Y_2O_3 was soluble in the garnet. Geller[36] discussed a possible mechanism of the solid solution in the garnet structure that may involve vacancies or vacancy–interstitial complexes instead of substitutional atoms. Neiman *et al.*[14] reported that the YAG structure can exist with some deficit of Al_2O_3. Several studies (see, for example, Toolenaar and de With[47] and Mulder and de With[48]) also have identified Al_2O_3 inclusions in YAG ceramics. In this work, we intend to find the most probable mechanism of accommodating the deviations from stoichiometry in YAG structure.

For excess Y_2O_3 in YAG, we can write the following equations that involve the formation of vacancies, interstitials, and antisites:
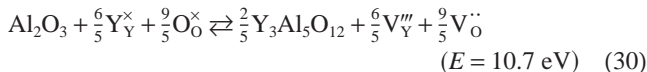
$$Y_2O_3 + 2Al_{Al(a)}^\times \rightleftarrows 2Y_{Al(a)}^\times + Al_2O_3 \qquad (E = 0.5 \text{ eV}) \qquad (17)$$

$$Y_2O_3 \rightleftarrows 2Y_i^{\cdot\cdot\cdot} + 3O_i'' \qquad (E = 36.2 \text{ eV}) \qquad (18)$$

$$Y_2O_3 + 2Al_{Al(a)}^\times + 3O_O^\times \rightleftarrows 2YAlO_3 + 2V_{Al(a)}''' + 3V_O^{\cdot\cdot} \qquad (E = 23.3 \text{ eV}) \quad (19)$$

$$Y_2O_3 + \tfrac{2}{3}Al_{Al(a)}^\times \rightleftarrows \tfrac{1}{3}Y_3Al_5O_{12} + Y_{Al(a)}^\times + \tfrac{2}{3}V_{Al(a)}''' + V_O^{\cdot\cdot} \qquad (E = 7.4 \text{ eV}) \quad (20)$$

$$Y_2O_3 + \tfrac{1}{2}Al_{Al(a)}^\times + \tfrac{3}{4}Al_{Al(d)}^\times \rightleftarrows \tfrac{1}{4}Y_3Al_5O_{12} + \tfrac{5}{4}Y_{Al}^\times \qquad (E = -0.3 \text{ eV}) \quad (21)$$

$$Y_2O_3 + \tfrac{1}{2}Al_{Al(a)}^\times + \tfrac{3}{4}Al_{Al(d)}^\times \rightleftarrows \tfrac{1}{4}Y_3Al_5O_{12} + \tfrac{5}{4}Y_i^{\cdot\cdot\cdot} + \tfrac{1}{2}V_{Al(a)}''' + \tfrac{3}{4}V_{Al(d)}''' \qquad (E = 9.4 \text{ eV}) \quad (22)$$

$$Y_2O_3 + \tfrac{4}{3}Al_{Al(a)}^\times + 2Al_{Al(d)}^\times + 5O_O^\times \rightleftarrows \tfrac{2}{3}Y_3Al_5O_{12} + \tfrac{4}{3}V_{Al(a)}'''$$
$$+ 2V_{Al(d)}''' + 5V_O^{\cdot\cdot} \qquad (E = 38.1 \text{ eV}) \quad (23)$$

E is the calculated enthalpy of the given reaction.

Quite similarly, we can describe the accommodation of an Al_2O_3 excess:

$$Al_2O_3 + 2Y_Y^\times \rightleftarrows 2Al_Y^\times + Y_2O_3 \qquad (E = 2.9 \text{ eV}) \qquad (24)$$

$$Al_2O_3 \rightleftarrows 2Al_i^{\cdot\cdot\cdot} + 3O_i'' \qquad (E = 52.5 \text{ eV}) \qquad (25)$$

$$Al_2O_3 + 2Y_Y^\times + 3O_O^\times \rightleftarrows 2YAlO_3 + 2V_Y''' + 3V_O^{\cdot\cdot} \qquad (E = 18.9 \text{ eV}) \qquad (26)$$

$$Al_2O_3 + Y_Y^\times + O_O^\times \rightleftarrows \tfrac{1}{3}Y_3Al_5O_{12} + Al_Y^\times + \tfrac{2}{3}V_Y''' + V_O^{\cdot\cdot} \qquad (E = 5.7 \text{ eV}) \quad (27)$$

$$Al_2O_3 + \tfrac{5}{4}Y_Y^\times \rightleftarrows \tfrac{1}{4}Y_3Al_5O_{12} + \tfrac{5}{4}Al_Y^\times \qquad (E = 0.2 \text{ eV}) \qquad (28)$$

$$Al_2O_3 + \tfrac{3}{4}Y_Y^\times \rightleftarrows \tfrac{1}{4}Y_3Al_5O_{12} + \tfrac{3}{4}Al_i^{\cdots} + \tfrac{3}{4}V_Y''' \qquad (E = 7.6 \text{ eV})$$
(29)

$$Al_2O_3 + \tfrac{6}{5}Y_Y^\times + \tfrac{9}{5}O_O^\times \rightleftarrows \tfrac{2}{5}Y_3Al_5O_{12} + \tfrac{6}{5}V_Y''' + \tfrac{9}{5}V_O^{\cdot\cdot}$$
$$(E = 10.7 \text{ eV}) \quad (30)$$
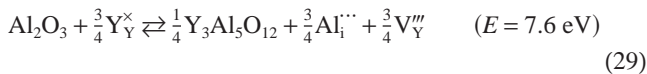
Inspection of the list of reactions and energies reveals that only reaction (21) has a negative energy and, therefore, is exothermic. This observation leads to the conclusion that the antisite substitution of $Y_{Al(a)}^\times$ is the most favorable of all the possible mechanisms of accommodation of extra Y cations in the YAG structure. This energy is comparable to that of reaction (17), which describes $Y_{Al(a)}^\times$ antisite formation that is accompanied by Al_2O_3 segregation and shows a very small (endothermic) reaction enthalpy, which indicates a high probability of its occurrence. Therefore, Al_2O_3 inclusion formations[47,48] may be stimulated by a Y_2O_3 surplus in YAG. An Al_2O_3 deficit in the garnet structure, which was postulated by Neiman *et al.*,[14] indeed can exist in YAG. Comparison of reactions (21) and (28) indicates that the $Y_{Al(a)}^\times$ antisite formation in Y_2O_3-rich YAG is slightly more preferable than the $Al_Y^\times$ formation in Al_2O_3-rich YAG, although the latter is still possible, because of the small enthalpy of the process. In addition, these reactions indicate that extra Y cations can be accommodated in the YAG lattice earlier than Al cations. This fact has been proven experimentally; for example, a Y_2O_3 excess of up to 2% was reported, while an Al_2O_3 surplus in YAG was observed only up to 0.5% (see, for instance, Sakaguchi *et al.*[18]).

The formation of defect complexes, such as an interstitial and the corresponding vacancy (see reactions (22) and (29)), requires much more energy, with respect to the antisite formation (reactions (21) and (28)). The energy required for the formation of interstitial defects, which has been described by reactions (18) and (25), also is very high, which is expected from Frenkel disorder energetics (see Section III*(2)*). The segregation in the perovskite-like phase in YAG (reactions (19) and (26)) also is expected to have a low probability, because the reaction has a very high energy.

Reaction (20) represents a mechanism of the defect accommodation that is predicted by Neiman *et al.*,[14] and reaction (27) has been constructed by analogy. Reactions (23) and (30) describe the process that was suggested by Sakaguchi *et al.*[18] Our calculations indicate that neither of these mechanisms are predicted to occur in YAG crystal. The calculated results imply that the defect equilibrium in an excess material has a different nature than that which has been considered in these studies. Neither an excess of Y_2O_3 nor Al_2O_3 seems to be the source of oxygen vacancies in pure YAG. However, interactions between defects were not included in the present study; this mechanism may be important under the conditions of large deviations from stoichiometry in materials.

IV. Conclusions

In the present theoretical study, atomistic calculations of the formation of native point defects in yttrium aluminum garnet (YAG) crystal are performed. Schottky and Frenkel defect formation energies are calculated, as well as antisite substitutions in the cation sublattice. The calculated results indicate the following:

(1) Intrinsic disorder in stoichiometric YAG is dominated by antisites.

(2) Antisite $Y_{Al(a)}^\times$ substitution causes a distortion in the crystalline lattice, which shortens the Y–O bond length, whose calculated value is in excellent agreement with the extended X-ray absorption fine-structure (EXAFS) measurements.

(3) A Y_2O_3 excess is energetically more favorable than an Al_2O_3 surplus in YAG.

(4) The formation of antisite disorder in YAG with excess Y_2O_3 or Al_2O_3 is the most probable mechanism of accommodating deviations from stoichiometry.

APPENDIX

Table A-I shows the interionic potential and shell parameter sets of Schuh *et al.*[17] and Bush *et al.*[40] Table A-II gives basic isolated defect formation energies that have been obtained using these parameter sets, in addition to the set that we have derived in this study.

One of the most important advantages of the shell model is a correct description of the optical modes of vibration and, as a result, a correct value of the high-frequency dielectric constant. As shown previously in Section III*(2)*, this value may be sensitive to the treatment of the polarization of cations in the model.

We now can analyze the influence of polarization on the defect formation energy. Schottky-like and Frenkel disorder energies in the YAG structure have been collected in Table A-III; this compilation shows that the choice of potential does not change the main conclusion regarding the preference of disorder in YAG. However, more-careful examination of the energetics of the reactions reveals some sort of contradiction. The formation of Frenkel Y defects (reaction (13)) demands the highest energy, using the Schuh set, whereas, using Bush parameters, Frenkel Al(d) defects (reaction (12)) have the highest energy. The lowest energy among cation Frenkel pairs corresponds to Al(d) pair formation in the Schuh set, which contrasts that obtained from the Bush results.

Furthermore, the probability of Al_2O_3 and Y_2O_3 segregation (reactions (9) and (10)) is comparable, using the Schuh set. The Bush set predicts a large difference between these reactions. Also, the Bush parameters indicate that Y_2O_3 segregation is only 1.1–0.4 eV less favorable than antisite-pair formation (reactions (15) and (16)), which contrasts the Schuh results.

The results lead to the conclusion that the defect formation energy is very sensitive to the treatment of polarization effects in the lattice. Therefore, to obtain accurate results regarding the energetics of the defect formation in YAG, one should carefully consider the polarization of ions in the lattice.

Table A-I.   Interatomic Potential Parameters and Shell Constants from Studies by Schuh *et al.*[17] and Bush *et al.*[40]†

Ion interaction	A (eV)	ρ (Å)	C (eV/Å^6)	Y^+ (|e|)	K^+ (eV/Å^2)
		Schuh *et al.*[17]			
O^{2-}–O^{2-}	22764.000	0.149	27.88	0.8481	74.92
Y^{3+}–O^{2-}	1345.1	0.3491	0.0	−0.251	71.70
Al^{3+}–O^{2-}	1469.3	0.2991	0.0	3.00	
		Bush *et al.*[40]			
O^{2-}–O^{2-}	25.41	0.6937	32.32	0.513	20.53
Y^{3+}–O^{2-}	1519.279	0.3291	0.0	3.00	
Al^{3+}–O^{2-}	2409.505	0.2649	0.0	0.043	403.98

†See footnote in Table I for a description of parameters A, ρ, C, Y^+, and K^+.

Table A-II.　Defect Energies of Intrinsic Defects in YAG, Obtained Using Different Parameter Sets

Type of defect	Formation energy (eV)		
	Present study	Schuh	Bush
Vacancy			
O	21.54	22.35[†]	17.63
Y	49.42	46.5[†]	47.74
Al, a-site (Al(a))	53.76	60.24[†]	59.94
Al, d-site (Al(d))	53.44	58.9[†]	65.10
Interstitial			
O(g) ($\frac{1}{8},x,\frac{1}{4}$-$x$)	−11.38	−11.35	−8.33
O(f) (x,0,$\frac{1}{4}$)	−11.79	−11.06	−7.84
Y(b) ($\frac{1}{8},\frac{1}{8},\frac{1}{8}$)	−36.85	−25.62[†]	−33.51
Al(b) ($\frac{1}{8},\frac{1}{8},\frac{1}{8}$)	−40.72	−45.1[†]	−47.48
Antisite			
Al in Y site	−0.69	−10.45	−8.93
Y in Al(a) site	2.38	13.53	11.52
Y in Al(d) site	4.16	14.29	12.78

[†]Value taken from the work of Schuh *et al.*[17]

Table A-III.　Reaction Energies (per Defect) for Schottky-like, Frenkel, and Antisite Disorder Reactions, Obtained Using Different Parameter Sets

Reaction	Reaction energy (eV)		
	Present study	Schuh	Bush
Schottky-like			
$3V'''_Y + 5V'''_{Al} + 12V^{\cdot\cdot}_O$ (reaction (8))	4.26	5.32[†]	3.41
$Al_2O_3 + 2V'''_{Al} + 3V^{\cdot\cdot}_O$ (reaction (9))	4.70	4.93	4.07
$Y_2O_3 + 2V'''_Y + 3V^{\cdot\cdot}_O$ (reaction (10))	3.88	4.91	2.40
$YAlO_3 + V'''_Y + V'''_{Al} + 3V^{\cdot\cdot}_O$ (reaction (11))	4.21		
Frenkel			
$V'''_{Al(a)} + Al^{\cdot\cdot\cdot}_i$ (reaction (12))	6.65	7.57[†]	6.23
$V'''_{Al(d)} + Al^{\cdot\cdot\cdot}_i$ (reaction (12))	6.36	6.88[†]	8.81
$V'''_Y + Y^{\cdot\cdot\cdot}_i$ (reaction (13))	6.28	10.44[†]	7.12
$V^{\cdot\cdot}_O + O''_{i(g)}$ (reaction (14))	5.08	5.50	4.65
$V^{\cdot\cdot}_O + O''_{i(f)}$ (reaction (14))	4.88	5.65	4.90
Antisite pair			
$Y^{\cdot\cdot}_{Al(a)} + Al^\times_Y$ (reaction (15))	0.9	1.54	1.30
$Y^{\cdot\cdot}_{Al(d)} + Al^\times_Y$ (reaction (16))	1.8	1.92	1.95

[†]Value taken from the work of Schuh *et al.*[17]

References

[1]T. A. Parthasarathy, T. Mah, and L. E. Matson, "Creep Behavior of an Al_2O_3–$Y_3Al_5O_{12}$," *Ceram. Eng. Sci. Proc.*, **11**, 1628 (1990).

[2]V. F. Kitaeva, N. N. Sobolev, I. L. Chistyj, E. V. Zharikov, V. V. Osiko, M. I. Timoshechkin, and A. C. Zolot'ko, "Molecular Light Scattering in Garnets," *Sov. Solid State Phys.*, **22** [5] 1379 (1980).

[3]S. R. Rotman, "Comment on 'Optical and Electron Paramagnetic Resonance Studies of Fe Impurities in Yttrium Aluminum Garnet Crystals'," *Phys. Rev. B: Condens. Matter*, **41** [1] 791–92 (1990).

[4]S. R. Rotman, H. L. Tuller, and C. Warde, "Defect–Property Correlations in Garnet Crystals. VI. The Electrical Conductivity, Defects Structure, and Optical Properties of Luminescent Calcium and Cerium-Doped Yttrium Aluminum Garnet," *J. Appl. Phys.*, **71** [3] 1209–14 (1992).

[5]Y. B. Rozenfeld and S. R. Rotman, "The Luminescence of Defects in Yttrium Aluminum Garnet," *Phys. Status Solidi A*, **139** [1] 249–62 (1993).

[6]A. Sugimoto, Y. Nobe, and K. Yamagishi, "Crystal Growth and Optical Characterization of Cr,Ca:$Y_3Al_5O_{12}$," *J. Cryst. Growth*, **140**, 349–54 (1994).

[7]G. I. Vetrogon, V. I. Danilenko, V. Ya. Kabanchenko, V. V. Osiko, A. M. Prohorov, A. N. Terent'evskij, and M. I. Timoshechkin, "EPR Spectra of Cr^{3+} Ion in Yttrium Aluminum Garnet," *Sov. Solid State Phys.*, **22** [11] 3216 (1980).

[8]D. Massiot, C. Bessada, J. P. Countures, and F. Tauelle, "A Quantitative Study of Al MAS NMR in Crystalline YAG," *J. Magn. Reson.*, **90**, 231–42 (1990).

[9]S. M. Zhilyakov, V. I. Mal'cev, and E. P. Naiden, "Magnet Structure Y-Fe-Sc Garnets," *Sov. Solid State Phys.*, **22** [5] 1388–93 (1980).

[10]G. R. Asatryan, G. P. Baranov, and V. I. Zhekov, "Electron Paramagnetic Resonance of Dy^{3+} Ions in YAG," *Sov. Solid State Phys.*, **38** [3] 814–21 (1996).

[11]J. Kumar, M. Thirumavalavan, R. Dhanasekaran, F. D. Gnanam, and P. Ramasamy, "Thermodynamics and Nucleation Behaviour in the System Y_2O_3–Al_2O_3–$Y_3Al_5O_{12}$," *J. Phys. D: Appl. Phys.*, **19**, 1223–31 (1986).

[12]N. H. Kim, Q. D. Fun, K. Komeya, and T. Meguro, "Phase Reaction and Sintering Behavior in the Pseudoternary System AlN–Y_2O_3–Al_2O_3," *J. Am. Ceram. Soc.*, **79** [10] 2645–51 (1996).

[13]W. R. Blumenthal and D. S. Philips, "High-Temperature Deformation of Single-Crystal Yttrium–Aluminum Garnet (YAG)," *J. Am. Ceram. Soc.*, **79** [4] 1047–52 (1996).

[14]A. Ya. Neiman, E. V. Tkachenko, and V. M. Zhukovskii, "Nature of Defect Formation in Complex Oxides of the Composition $Me_3E_5O_{12}$ with a Garnet Structure," *Dokl. Akad. Nauk SSSR*, **240**, 876–79 (1978).

[15]H. Haneda, Y. Miyazawa, and S. Shirasaki, "Oxygen Diffusion in Single Crystal Yttrium Aluminum Garnet," *J. Cryst. Growth*, **68** [2] 581–88 (1984).

[16]L. Schuh, R. Metselaar, and G. de With, "Electrical Transport and Defect Properties of Ca- and Mg-Doped Yttrium Aluminum Garnet Ceramics," *J. Appl. Phys.*, **66** [N6] 2627 (1989).

[17]L. Schuh, R. Metselaar, and C. R. A. Catlow, "Computer Modelling Studies of Defect Structures and Migration Mechanisms in Yttrium Aluminum Garnet," *J. Eur. Ceram. Soc.*, **7**, 67–74 (1991).

[18]I. Sakaguchi, H. Haneda, J. Tanaka, and T. Yanagitani, "Effect of Composition on the Oxygen Tracer Diffusion in Transparent Yttrium Aluminum Garnet (YAG) Ceramics," *J. Am. Ceram. Soc.*, **79** [6] 1627–32 (1996).

[19]M. Kh. Ashurov, Yu. K. Voronko, V. V. Osiko, A. A. Sobol, and M. I. Timoshechkin, "Spectroscopic Study of Stoichiometry Deviation in Crystals with Garnet Structure," *Phys. Status Solidi A*, **42**, 101 (1977).

[20]C. Landron, S. Lefloch, M. Gervais, J. P. Coutures, and D. Bazin, "Yttrium Coordination Shell in YAG Related Structures," *Phys. Status Solidi B*, **196**, 25 (1996).

[21]H. Donnerberg and C. R. A. Catlow, "Atomistic Computer Simulations of Yttrium Iron Garnet (YIG) as an Approach to Studying Its Defect Chemistry: I. Intrinsic Defects," *J. Phys.: Condens. Matter*, **5**, 2947 (1993).

[22]C. R. A. Catlow and R. James, "Defect Energetics in α-Al_2O_3 and Rutile TiO_2," *Phys. Rev. B*, **25** [2] 1006–26 (1982).

[23]C. R. A. Catlow, *Proc. R. Soc. London, A*, **353**, 533 (1977).

[24]A. B. Lidiard and M. J. Norgett, *Computational Solid State Physics*; p. 385. Plenum Press, New York, 1972.

[25]M. J. Nogett, Atomic Energy Research Establishment Report No. AERE R7605, Harwell, U.K., 1972.

[26]R. A. Buckingham, *Proc. R. Soc., A*, [168] 264 (1938).

[27]N. F. Mott and M. J. Littleton, "Conduction in Polar Crystals: Electrolytic Conduction in Solid Salts," *Trans. Faraday Soc.*, **34**, 485 (1938).

[28]B. G. Dick and A. W. Overhauser, "Theory of the Dielectric Constant of Alkali Halide Crystals," *Phys. Rev.*, **112**, 90 (1958).

[29]G. Menzer, "Die Kristallstruktur von Granat," *Z. Kristallogr.*, **63**, 157–58 (1926).

[30]G. Menzer, "Die Kristallstruktur der Granate," *Z. Kristallogr.*, **69**, 300–96 (1928).

[31]I. F. Bikmetov, A. B. Sobolev, V. A. Lobach, A. I. Mit'kovets, A. A. Starov, and A. P. Shkadarevich, "Electronic Structure of Cr^{4+} Ions in Yttrium-Aluminum Garnet in the Embedded Cluster Approximation," *J. Appl. Spectrosc.*, **53** [N6] 1315–18 (1990).

[32]H. Donnerberg and C. R. A. Catlow, "Atomistic Computer Simulations of Yttrium Iron Garnet as an Approach to Studying Its Defect Chemistry: Extrinsic Defects," *Phys. Rev. B: Condens. Matter*, **50** [2] 744–50 (1994).

[33]R. W. G. Wyckoff, *Crystal Structures,* Vol. 3; p. 967. Wiley, New York, London, U.K., and Sydney, Australia, 1965.

[34]E. Prince, "Neutron Diffraction Measurements on Yttrium-Iron and Yttrium-Aluminum Garnets," *Acta Crystallogr.*, **10**, 787–88 (1957).

[35]F. Euler and J. A. Bruce, "Oxygen Coordinates of Compounds with Garnet Structure," *Acta Crystallogr.*, **19**, 971–78 (1965).

[36]S. Geller, "Crystal Chemistry of the Garnets," *Z. Kristallogr.*, **125**, 1–47 (1967).

[37]M. Z. Keith and R. Roy, "Structural Relations among Double Oxides of Trivalent Elements," *Am. Mineral.*, **39**, 1–23 (1954).

[38]G. V. Lewis and C. R. A. Catlow, *J. Phys. C: Solid State Phys.*, **18**, 1149–61 (1985).

[39]J. D. Gale, "General Utility Lattice Program," *J. Chem. Soc. Faraday Trans.*, **93**, 629 (1997).

[40]T. S. Bush, J. D. Gale, C. R. A. Catlow, and P. D. Battle, "Self-Consistent Interatomic Potentials for the Simulation of Binary and Ternary Oxides," *J. Mater. Chem.*, **4** [6] 831–37 (1994).

[41]G. V. Lewis and C. R. A. Catlow, "Defect Studies of Doped and Undoped Barium Titanate Using Computer Simulation Techniques," *J. Phys. Chem. Solids*, **47** [1] 89–97 (1986).

[42]S. Geller and E. A. Wood, "Crystallographic Studies of Perovskite-like Compounds, I. Rare Earth Orthoferrites and $YFeO_3$, $YCrO_3$, $YAlO_3$," *Acta Crystallogr.*, **9**, 563 (1956).

[43]S. Geller and V. B. Bala, "Crystallographic Studies of Perovskite-like Compounds, II. Rare Earth Aluminates," *Acta Crystallogr.*, **9**, 1019 (1956).

[44]Landolt-Börnstein, "Group III: Crystal and Solid State Physics"; in *Numerical Data and Functional Relationship in Science and Technology, New Series, Vol. 7.* Springer–Verlag, Berlin–Heidelberg–New York, 1969.

[45]F. A. Kröger and H. J. Vink, *Solid State Physics 3*. Edited by F. Seitz and F. Turnbull. Academic Press, New York, 1956.

[46]D. A. Bonnell; private communication, 1997.

[47]F. J. C. Toolenaar and G. de With, *Proc. Br. Ceram. Soc.*, **37**, 241 (1986).

[48]C. A. M. Mulder and G. de With, "Translucent $Y_3Al_5O_{12}$ Ceramics: Electron Microscopy Characterisation," *Solid State Ionics*, **16**, 87 (1985).

[49]V. F. Kitaeva, E. V. Zharikov, and I. L. Chistyi, *Phys. Status Solidi A*, **92**, 475–88 (1985).

[50]K.-H. Hellwege (ed.), "Group II, Crystal and Solid State Physics"; in *Numerical Data and Functional Relationship in Science and Technology, New Series, Vol. 2.* Springer–Verlag, Berlin, FRG, Heidelberg, FRG, and New York, 1969.　□